Indonesian Journal of Maritime Technology (ISMATECH)
Vol. 04, Issue 01, June 2026
eISSN: 3025-518X
DOI: https://doi.org/10.35718/ismatech.v4i1.8482002

Structural Response and Optimization of a Tugboat Midship Section Under Varied Transverse Frame Spacing Using Finite Element Analysis

Amalia Ika Wulandari[1)*], Alamsyah [1)], Hariyono[1)], Ryan Raruk[1)], Husein Syahab[1)], Muhammad Anjas Syam[1)], Suardi[1)], Dimas Fajar Prasetyo[2)]

[1]Department of Naval Engineering, Institut Teknologi Kalimantan, Balikpapan, Indonesia
[2]School of Earth and Oceans, The University of Western Australia, Australia

KEYWORDS
Tugboat;
Midship Section;
Frame Spacing;
Von Mises Stress;
Deformation

ABSTRACT – Transverse framing systems serve as a critical structural backbone for marine vessels, governing localized stiffness and cross-sectional hull strength. This study investigates the structural response of a tugboat's midship section under various transverse frame spacing configurations using the Finite Element Method (FEM) to optimize lightweight tonnage (LWT) while maintaining seaworthiness. Utilizing structural data from a under-30-meter service tugboat, five distinct frame spacing variations 500 mm (baseline actual design), 550 mm, 575 mm, 600 mm, and 625 mm were modeled using four-node shell elements (SHELL181) within ANSYS software. A constant uniform static deck pressure load of 0.0122 MPa was applied to evaluate localized stress distributions and elastic displacement fields under rigid boundary conditions. Numerical simulations reveal a progressive, linear increase in both equivalent stresses and vertical deflections as the unsupported span of the deck plating expands. The maximum von Mises equivalent stress escalated from 31.4237 MPa at the 500 mm baseline configuration to 34.1552 MPa (550 mm), 35.4687 MPa (575 mm), 36.8590 MPa (600 mm), and peaked at 40.6607 MPa under the widest 625 mm spacing. Concurrently, the total displacement vector sum rose from 0.56047 mm at the baseline to a peak of 0.86030 mm at 625 mm spacing due to the reduction of localized flexural rigidity. Crucially, despite the elevated structural responses, all configurations safely satisfy the strict structural limits enforced by the Indonesian Classification Bureau (BKI 2022) rules, as the maximum peak stress (40.6607 MPa) remains substantially below the nominal upper yield strength of ordinary hull structural steel (ReH = 235 N/mm^2). These findings demonstrate that extending the transverse frame spacing up to 625 mm is structurally viable, offering a verified mechanism for weight optimization without compromising structural safety margins.

*Corresponding Author | Amalia Ika Wulandari | ✉ (amaliaikaw@lecturer.itk.ac.id)

INTRODUCTION

Tugboats, commonly known as tugs, are specialized marine vessels designed to assist larger ships during maneuvering, berthing, unberthing, and towing operations within ports, offshore areas, or narrow rivers [1]. Despite their relatively small size, tugboats possess high power-to-displacement ratios and are structurally engineered to withstand extreme vibrations and heavy operational loads while pulling or pushing vessels with significantly larger mass [2]. Given their demanding operational environment, maintaining the structural integrity of the hull against dynamic impacts and cyclic loading is paramount to ensure maritime safety and longevity [3], [4].

The hull structure of a ship primarily consists of essential structural members, where the framing system serves as the backbone of the vessel's cross-sectional geometry [5]. The framing system plays a critical role in governing the transverse strength, buckling resistance, and overall stiffness of the hull structure [6]. Therefore, determining the optimal frame spacing is vital to ensure an even distribution of operational loads across the ship's structure, thereby mitigating the risk of localized structural failure or catastrophic hull collapse [7]. Recent research emphasizes that optimizing frame geometry directly enhances the ultimate strength of local panels under severe pressure [8].

The primary challenge in modern ship design is to engineer a framing system that provides a robust and rigid structure while minimizing lightweight tonnage (LWT) to optimize fuel efficiency and deadweight capacity [9].

However, any weight reduction strategy must strictly adhere to the regulations set by classification societies, such as the Indonesian Classification Bureau (Biro Klasifikasi Indonesia/BKI) [5]. In structural evaluation, the maximum allowable stress, fatigue limits, and bending moment criteria defined by BKI standards serve as the baseline requirements for assessing ship strength and ensuring seaworthiness [10]. To achieve this, advanced multi-objective optimization models are frequently employed to balance weight minimization with strict safety margins [11].

Traditional structural design and analysis can be resolved through analytical and mathematical approaches. However, traditional mathematical methods become highly complex, time-consuming, and impractical when dealing with irregular geometries and non-uniform load distributions inherent in ship structures [12]. To overcome this limitation, numerical approaches like the Finite Element Method (FEM) are widely utilized in modern naval architecture [13]. FEM is a numerical technique that discretizes a continuous structure into smaller, interconnected subregions known as finite elements, enabling the analysis of complex structures with higher accuracy and computational efficiency [12].

By implementing FEM, the distribution of localized stress, deformation patterns, and safety factors of the tugboat can be evaluated accurately under various operational scenarios, facilitating effective design optimizations before the physical construction phase [14]. Furthermore, computational simulations allow designers to evaluate the progressive collapse behavior of deck plating and stiffeners when subjected to localized concentrated loads [15].

While several studies have evaluated global hull strength under wave loads, research specifically addressing the localized structural response of tugboat decks under varied frame spacing remains limited. Therefore, this study aims to investigate the direct correlation between frame spacing variations and the resulting local stress, deformation, and safety factors. The analysis focuses specifically on the midship section of a tugboat under 30 meters in length, subjected strictly to deck loading conditions. By analyzing five distinct frame spacing configurations—500 mm, 550 mm, 575 mm, 600 mm, and 625 mm—using FEM software, this research provides critical insights into identifying structural hotspots and optimizing the structural design of small-scale service vessels.

METHODS

Ship Data and Modelling

This section outlines the systematic steps undertaken to evaluate the impact of frame spacing variations on the structural strength of a tugboat's midship section. The research combines empirical data collection, compliance with classification society rules, and numerical simulations using Finite Element Method (FEM) software.

The initial phase involved a comprehensive literature review to establish a robust theoretical foundation regarding ship midship sections, transverse framing systems, and structural mechanics. This phase encompassed the evaluation of prior research, material science, and numerical analysis methodologies using computer-aided engineering (CAE) software, specifically ANSYS. Technical guidelines and regulatory frameworks established by the Indonesian Classification Bureau (Biro Klasifikasi Indonesia/BKI) were thoroughly reviewed to ensure standard compliance [5].

Thin Plate Theory and Shell Kinematics

To understand the structural response of the deck plating under localized loads, the research incorporates First-order Shear Deformation Theory (FSDT), often referred to as Mindlin-Reissner plate theory. Unlike classical thin plate theory (Kirchhoff-Love), FSDT accounts for transverse shear deformation through the thickness, which is critical for ship plating supported by stiff frames [16]. The displacement field (u, v, w) at any point in the shell is mathematically defined in Equations (1), (2), and (3).

$$u(x,y,z) = u_0(x,y) + z\theta_x(x,y) \quad (1)$$

$$v(x,y,z) = v_0(x,y) + z\theta_y(x,y) \quad (2)$$

$$w(x,y,z) = w_0(x,y) \quad (3)$$

Where u_0, v_0, w_0 are the mid-surface displacements, and θ_x, θ_y represent the rotations of the normal sections around the Y and X axes, respectively.

Data Collection

This study relies on secondary data obtained from approved ship design drawings and actual vessel operational data that conform to BKI regulations. Field observations were additionally conducted at the shipyard to inspect the actual baseline frame spacing and the physical layout of the transverse structural components. The secondary

data establishing the operational reference for the numerical analysis consists of the vessel's principal dimensions, as detailed in Table 1.

Table 1. Principle Dimension

No.	Parameter	Size (m)
1	LOA	29.30
2	LPP	29.00
3	Height (H)	3.80
4	Draft (T)	2.30
5	Breadth (B)	8.60

The collected geometric parameters serve as the structural baseline to generate five distinct midship section configurations with varied frame spacing lengths: 500 mm, 550 mm, 575 mm, 600 mm, and 625 mm.

Midship Section Modeling in ANSYS

The physical dimensions derived from the ship design drawings were transformed into three-dimensional numerical models within the ANSYS pre-processor. The structural modeling is governed by the following technical parameters:

I. Coordinate System: A 3D Cartesian coordinate system was implemented, where the positive X-axis represents the vessel's breadth (from portside to starboard), the positive Y-axis defines the ship's molded depth (from baseline to strength deck), and the Z-axis aligns with the longitudinal length of the ship.

II. Element Selection (SHELL181): The structural plating, frames, and longitudinal stiffeners were modeled using the SHELL181 element type. This four-node element is highly suitable for thin to moderately thick shell structures, featuring six degrees of freedom (DOFs) at each node (three translations and three rotations) [17]. It governs the linear stiffness matrix equation (4).

$$[K]\{u\} = \{F\} \tag{4}$$

Where [K] is the global structural stiffness matrix, {u} is the nodal displacement vector, and {F}is the applied load vector. This element enables accurate simulation of three-dimensional stress fields across the X, Y, and Z planes.

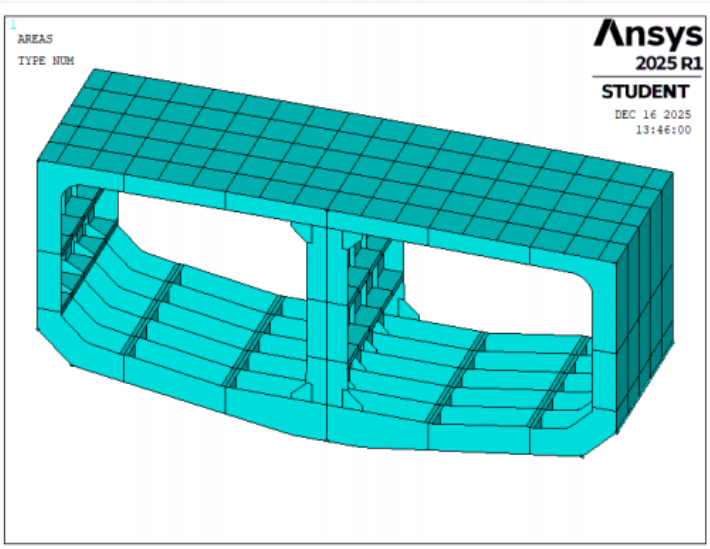

Figure 1. Geometric surface modeling of the tugboat midship section in ANSYS

The geometric surface configuration representing the midship section framework before mesh generation is illustrated in Fig. 1. To perform the numerical solution, the continuous geometric model was discretized into a finite element mesh network, as displayed in Fig. 2.

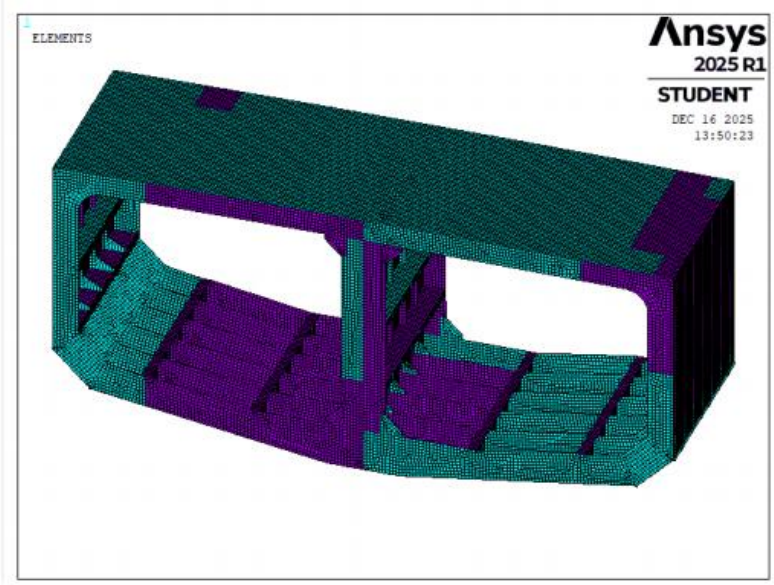

Figure 2. Finite element mesh generation using SHELL181 element

Fixed boundary conditions were applied at the neutral axis points of the ship's transverse structural components to simulate realistic constraints. The constraints applied at these nodes restricted all six degrees of freedom: translations (Ux = Uy = Uz = 0) and rotations (Rx = Ry = Rz = 0). Concurrently, the operational load was evenly distributed across the designated deck plate areas. The spatial distribution of the applied boundary conditions and external loads on the finite element model is visually demonstrated in Fig. 3.

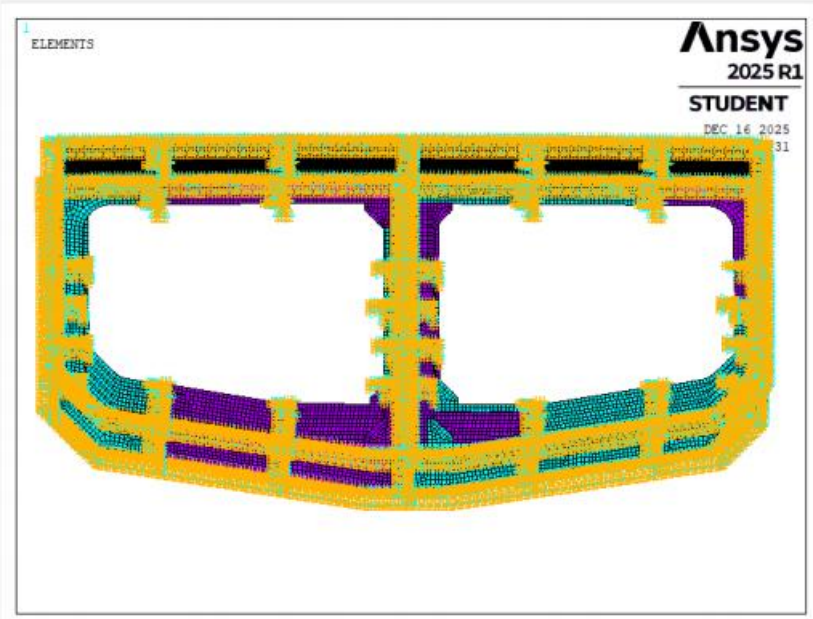

Figure 3. Application of multi-axial boundary conditions and localized deck loading

Midship Section Structural Testing

Numerical simulations were carried out to evaluate the structural response, localized stress distribution, and deformation trends of the midship section under specified deck loading conditions. Since the midship section experiences the most critical bending moments and cyclic pressures during operation—especially when navigating harsh wave environments—the finite element analysis (FEA) allows for the identification of potential structural hotspots, allowing for geometric optimization to maintain structural integrity.

To verify whether the structural designs meet the safety margins, the numerical results were compared against the nominal material properties specified by BKI 2022 rules [5]. The tugboat hull utilizes ordinary-strength hull structural steel, which possesses a minimum upper yield strength (R_{eH}) of 235 N/mm.

Von Mises Equivalent Stress Theory

Yielding criteria under multi-axial loading are evaluated using the Von Mises Equivalent Stress (σ_e) yield criterion [18]. The localized equivalent stress computed from the principal stresses ($\sigma_1, \sigma_2, \sigma_3$) must not exceed the allowable design limits, expressed in Equation (5).

$$\sigma_e = \sqrt{\frac{1}{2}[(\sigma_1 - \sigma_2)^2 + (\sigma_2 - \sigma_3)^2 + (\sigma_3 - \sigma_1)^2]} \quad (5)$$

Safety Factor Calculation

The structural safety factor (SF) for each frame spacing variation is calculated using the ratio of the material's yield strength to the maximum equivalent von Mises stress obtained from the FEM simulation, expressed in Equation (6).

$$SF = \frac{R_{eH}}{\sigma_{max}} \quad (6)$$

Where:

SF = Safety Factor
R_{eH} = Minimum yield strength of the material (235 N/mm)
σ_{max} = Maximum equivalent von Mises stress derived from the ANSYS simulation

RESULTS AND DISCUSSION

Geometric discretization, commonly referred to as meshing, represents a critical phase in Finite Element Method (FEM) analysis, transforming the continuous midship section structure of the tugboat into discrete elements. Because the quality and density of this mesh network significantly govern the numerical accuracy, convergence behavior, and computational efficiency of the subsequent simulations, a comprehensive mesh independence study was conducted on the 500 mm baseline model to ensure that the numerical solutions are free from discretization errors.

The evaluation systematically compared three levels of mesh refinement: coarse, medium, and fine configurations. As summarized in **Table 2**, upon refining the mesh framework from the medium to the fine level, the maximum equivalent von Mises stress exhibited a negligible discrepancy. The relative percentage variations between the medium and fine grids fall well within the strict acceptable tolerance threshold (under 2%), numerical convergence is fully verified. Consequently, the medium mesh density was selected as the optimal configuration to balance numerical accuracy with computational efficiency.

Table 2. Mesh Independence and Grid Convergence Study Results

Elements	Stress (Mpa)	Discrepancy (%)
550	29.85	
1378	31.42	5.27
3860	31.81	1.23

Utilizing this validated mesh configuration, the subsequent analysis evaluates the structural behavior of the tugboat's midship section under variations in frame spacing. To ensure consistency across all investigated frame configurations and simulate localized operational deck loading, a constant uniform static deck pressure load of 0.0122 MPa was systematically applied across all numerical models .calculated in accordance with the design load requirements for weather decks specified by Biro Klasifikasi Indonesia (BKI) 2022 Rules for Hull, Volume II, Section 4.

Structural Response of the 500 mm Frame Spacing Model (Baseline)

The 500 mm configuration represents the baseline model, reflecting the actual frame spacing of the vessel. The localized structural responses under the designated deck load are characterized below: Deformation

Characteristics: The finite element model generated a maximum displacement of 0.56047 mm, localized precisely at node 39485 shown in Figure 4.

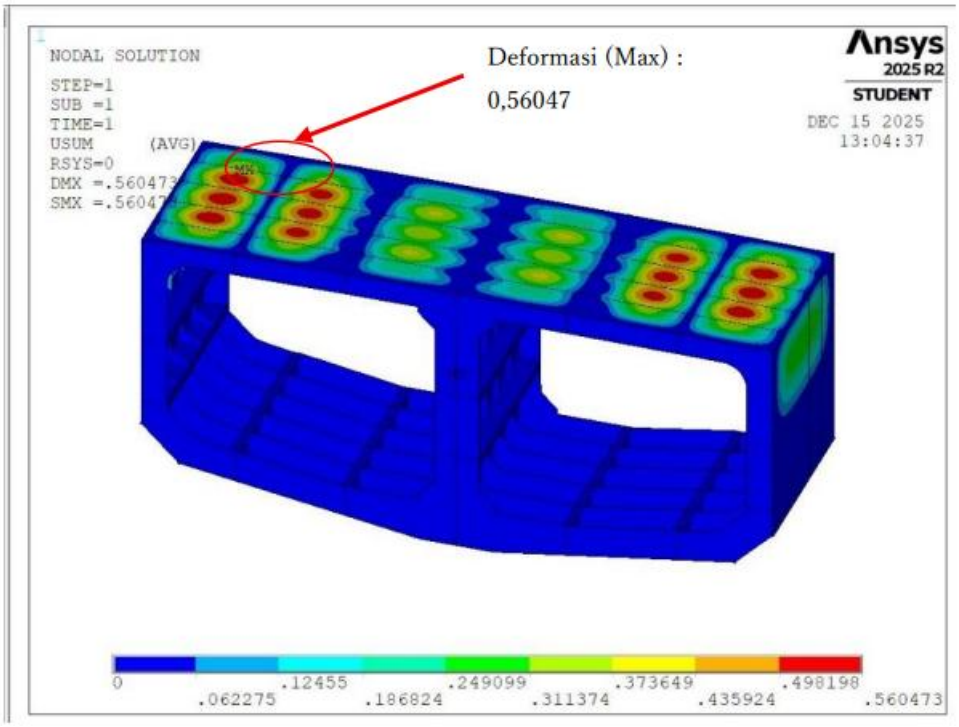

Figure 4. Total structural deformation contour of the deck plate with a 500 mm frame spacing

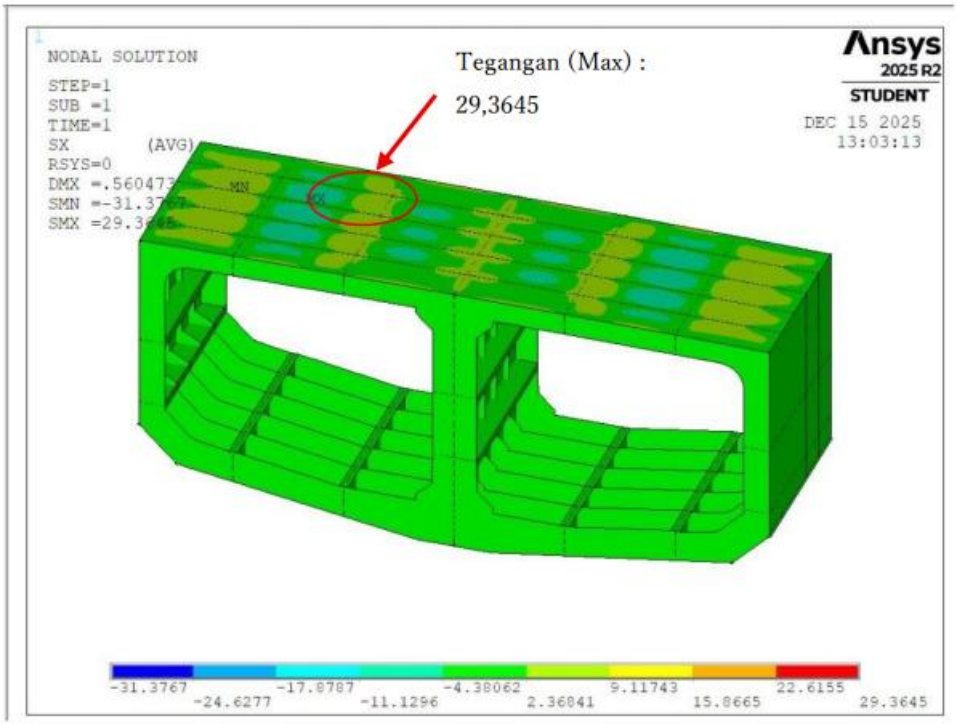

Figure 5. Normal stress distribution along the X-axis for the 500 mm frame spacing model.

The spatial deformation contour reveals that the highest displacement occurs along the free edges of the deck plating. Structurally, these regions exhibit lower bending stiffness due to the absence of rigid multi-axial boundary constraints. Multi-Axial Stress Component Response: The deck structure experiences distinct multi-axial normal stresses. The maximum localized directional stresses reached 29.3645 MPa along the X-axis (node 20515, Fig. 5), 24.6507 MPa along the Y-axis (node 5805, Fig. 6), and 19.3550 MPa along the Z-axis (node 44272, Fig. 7).

Equivalent Von Mises Stress: The combined multi-axial stress tensor was evaluated using the von Mises yield criterion (see Fig. 8). The peak equivalent stress reached 31.4237 MPa at node 20618, establishing the baseline yield reference. The compiled structural response data for the 500 mm frame spacing model are summarized in Table 4.1 and Table 4.2.

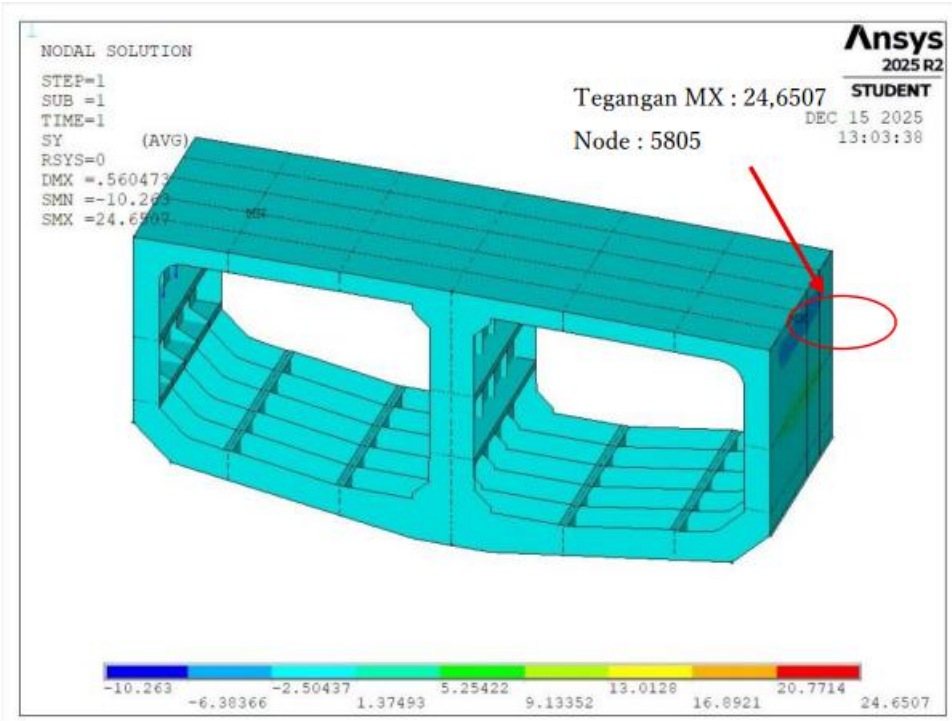

Figure 6. Normal stress distribution along the Y-axis for the 500 mm frame spacing model

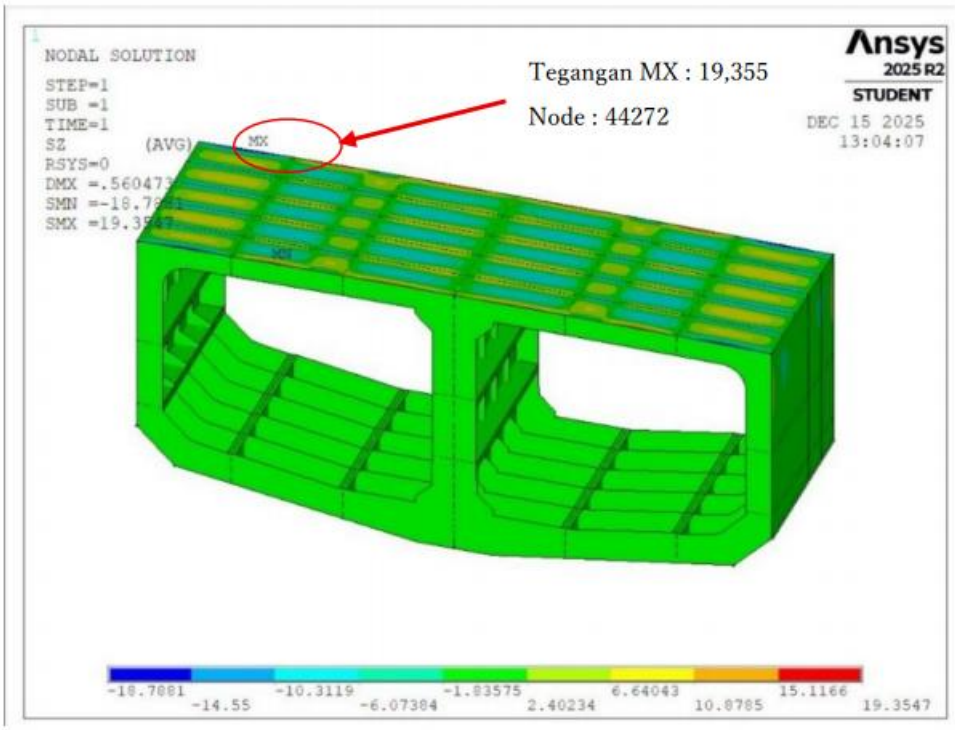

Figure 7. Normal stress distribution along the Z-axis for the 500 mm frame spacing model.

The finite element visualization models, as depicted in the respective contour plots (Fig. 4 to Fig. 8), provide a detailed spatial representation of the stress localization and structural deformation occurring within the tugboat's

midship section. These graphical figures illustrate how the structural plating and stiffener interfaces respond geometrically under the applied operational pressure.

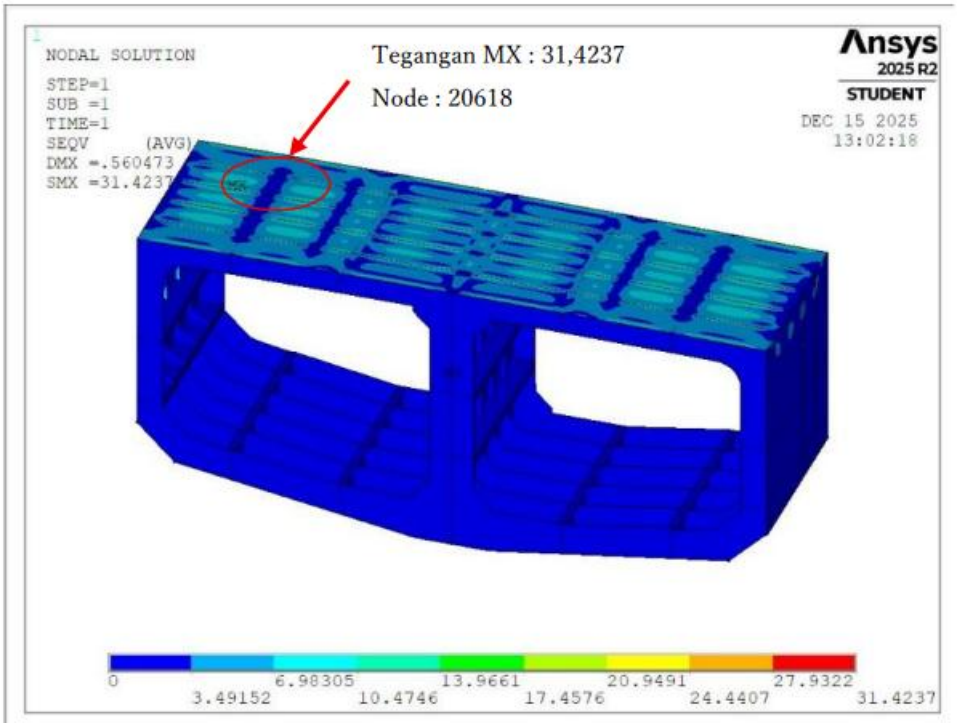

Figure 8. Equivalent von Mises stress contour for the 500 mm frame spacing model.

To analyze the mechanical trends systematically, a comprehensive cross-examination of these parameters across all investigated framing arrangements was performed. The numerical comparisons of the directional stresses, equivalent von Mises stresses, and total displacement vector sums for each specific frame spacing variant are compiled and presented in Table 2 and Figure 9.

Table 3. Consolidated Structural Responses Across All Investigated Frame Spacing Variations

Frame Spacing (mm)	Max σ_x (MPa)	Max σ_y (MPa)	Max σ_z (MPa)	Max Von Mises σ_e (MPa)	Critical Node (Stress)	Max Deformation (mm)	Critical Node (Deformation)
500 (Baseline)	293.645	246.507	193.550	314.237	20618	0.56	39485
550	311.977	266.298	215.853	341.552	16304	0.66	33889
575	324.987	277.454	231.010	354.687	17027	0.72	35200
600	337.920	288.560	242.330	368.590	16751	0.78	40827
625	427.183	128.092	290.813	406.607	44750	0.86	54127

The consolidated dataset presented in Table 2 reveals clear mechanical dependencies between the transverse framing intervals and the overall structural integrity of the tugboat's midship section. By evaluating the numerical progression from the baseline model to the widest variation, two primary behavioral trends emerge: a highly predictable linear escalation in elastic deformation, and a more complex, non-linear redistribution of multi-axial stress fields that shifts local load-bearing mechanisms.

Mechanics of Stress Redistribution and the 625 mm Structural Shifting. As the frame spacing is expanded from 500 mm to 600 mm, the equivalent von Mises stress (σe) exhibits a steady upward trend, rising from 31.4237 MPa to 36.8590 MPa. This linear growth strongly correlates with classical plate bending models where expanding the unsupported span increases the bending moment acting on individual plate panels under a constant lateral pressure [19]. The finite element visualization models depicted in the directional contour plots (Fig. 5, Fig. 6, and Fig. 7) illustrate how these stress vectors concentrate around the boundaries where the plate interfaces with the stiffeners. However, a significant mechanical shift occurs when the spacing is extended to 625 mm. At this specific threshold, the normal stress along the X-axis (σx) spikes dramatically by approximately 26% to 42.7183 MPa,

whereas the normal stress along the Y-axis (σy) drops sharply to 12.8092 MPa. This behavioral transition is highly indicative of a change in the plate's aspect ratio and localized boundary stiffness [20]. When the transverse frame spacing becomes excessively wide, the plate panel behaves less like a standard two-way bending member and instead transitions into a dominant one-way membrane tension field oriented along the vessel's breadth (X-axis) [21].

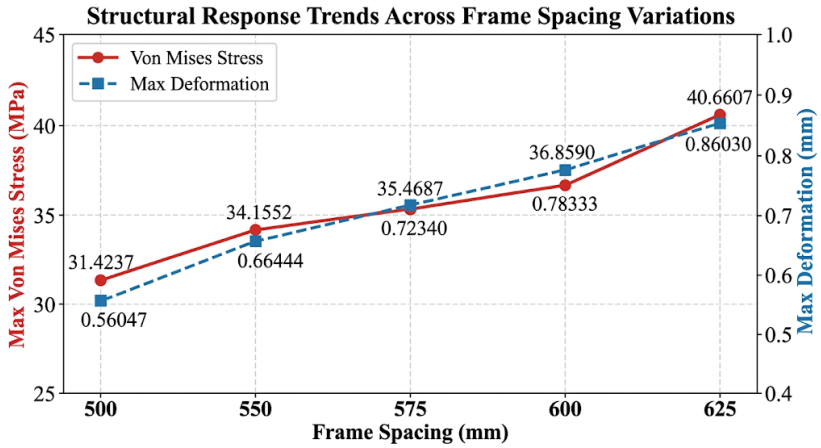

Figure 9. Comparison curve of maximum equivalent von Mises stress and maximum elastic deformation across different frame spacing variations.

The rigid longitudinal stiffeners absorb the primary structural constraints, causing the critical stress node to migrate to node 44750 (Fig. 8). This numerical migration proves that expanding the framing layout does not merely scale the stress values on fixed coordinates; it alters the fundamental mechanical load paths across the midship section [22].

Flexural Rigidity Degradation and Linear Deformation Escalation. In contrast to the non-linear shifts observed in directional stresses, the maximum displacement vector sum escalates in a strictly linear manner across all investigated spacing variations, as summarized in Table 2 and plotted in Fig. 9. According to classical thin-plate mechanics, the flexural rigidity of a shell structure is heavily dependent on the unsupported span length between rigid boundaries [23]. By widening the frame spacing from 500 mm to 625 mm, the local moment of inertia of the unstiffened deck panels drops significantly. This stiffness degradation results in a cumulative deflection penalty of roughly 53.5%, culminating in a peak deformation of 0.86030 mm at node 54127 (Fig. 4). The spatial deformation contours demonstrate that the highest displacement fields are consistently concentrated at the mid-span between transverse frames, validating that these specific unstiffened zones possess the lowest structural resistance to out-of-plane operational pressures [24].

Regulatory Safety Margins and Weight Optimization Feasibility. To validate the design feasibility of these structural variations, the empirical maximum stress values from Table 2 must be cross-referenced with international classification society regulations. Under the Biro Klasifikasi Indonesia (BKI) framework, the allowable design stress for ordinary hull structural steel is directly bounded by its upper yield limit (R_{eH} = 235 N/mm^2) [5]. Even under the most critical configuration (625 mm frame spacing), the peak equivalent von Mises stress of 40.6607 MPa utilizes only about 17.3% of the material's total yield capacity. This leaves a highly conservative safety factor (SF) of approximately 5.78, indicating that the entire midship section remains well within the safe elastic zone with no risk of plastic collapse or localized yielding failure [14]. From an economic and naval architecture standpoint, this massive structural reserve confirms that expanding the frame spacing to 625 mm is a viable design modification. Reducing the number of transverse frames over the ship's length optimizes the vessel's lightweight tonnage (LWT) [11]. This weight reduction directly cuts down manufacturing costs at the shipyard and improves operational fuel efficiency throughout the tugboat's service life, all while fully complying with classification safety standards [25].

CONCLUSION

Based on the finite element analysis (FEA) and comparative structural evaluation of the tugboat's midship section under varied transverse frame spacing configurations. Impact on Local Stress Fields: There is a direct, proportional correlation between the widening of the frame spacing and the elevation of localized equivalent stress within the deck plating. The baseline model (500 mm spacing) generated the minimum equivalent stress of 31.4237 MPa. Gradual widening of the frame spacing systematically increased the maximum von Mises stress to 34.1552 MPa for the 550 mm configuration, 35.4687 MPa for 575 mm, 36.8590 MPa for 600 mm, and reached a

peak stress concentration of 40.6607 MPa at the widest interval of 625 mm. Impact on Elastic Deformation: Expanding the unsupported spans between successive transverse frames directly compromises the local flexural rigidity of the strength deck panels, resulting in an upward linear trend in vertical deflection. The maximum structural displacement escalated from 0.56047 mm at the actual baseline spacing 500 mm to 0.66444 mm 550 mm), 0.72340 mm (575 mm), 0.78333 mm (600 mm), and ultimately culminated at a maximum displacement vector sum of 0.86030 mm under the 625 mm spacing configuration. Regulatory Compliance and Design Feasibility: Despite the noticeable increase in both stress concentration and elastic deformation as the frame intervals became wider, all analyzed configurations safely satisfy the strict structural safety margins defined by the Biro Klasifikasi Indonesia (BKI 2022) guidelines. The highest equivalent stress recorded 40.6607 MPa at 625 mm spacing) remains significantly below the minimum upper yield strength of ordinary hull structural steel (ReH = 235 N/mm^2). Consequently, extending the frame spacing up to 625 mm stands as a structurally viable option for small-scale service vessels under 30 meters, offering a verified pathway toward minimizing lightweight tonnage (LWT) and enhancing fuel efficiency without sacrificing seaworthiness or operational safety.

ACKNOWLEDGEMENT

The authors received no financial support or external funding for the research, authorship, and publication of this article. The entire study was conducted using self-funded resources and institutionally available infrastructure.

REFERENCES

[1] J. K. Paik, Ultimate Limit State Design of Steel-Plated Structures. Chichester, UK: Wiley, 2018.

[2] Xiong Y, Li C, Cai S, Wang D. The dynamic ultimate strength of stiffened panels under axial impact loading. Ships and Offshore Structures. 2023 May 4;18(5):707-20. doi; https://doi.org/10.1080/17445302.2022.2067417

[3] Abedin J. *Structural optimisation of ship hull using finite element method* (Doctoral dissertation, Newcastle University). doi; http://theses.ncl.ac.uk/jspui/handle/10443/6610

[4] Ma Z, Pei Z, Wu W. Dynamic ultimate strength analysis of stiffened plate based on Idealized Structural Unit Method. Marine Structures. 2022 Jul 1;84:103203. doi; https://doi.org/10.1016/j.marstruc.2022.103203

[5] Ilić N, Momčilović N. Progressive collapse analysis of inland waterway cargo vessel. Procedia Structural Integrity. 2023 Jan 1;48:318-25. doi; https://doi.org/10.1016/j.prostr.2023.07.126

[6] Biro Klasifikasi Indonesia (BKI), Rules for Hull, Volume II. Jakarta: BKI, 2022.

[7] Yang Y, Mu Z, Zhu B. Numerical Study on Elastic Buckling Behavior of Diagonally Stiffened Steel Plate Walls under Combined Shear and Non-Uniform Compression. Metals. 2022 Mar 31;12(4):600. doi; https://doi.org/10.3390/met12040600

[8] Pawara MU, Alamsyah A, Kusuma IP, Wulandari AI, Ikhwani RJ, Arifuddin MN. A Finite Element Analysis of Bottom Structure of LCT Converted from SPOB. Maritime Park: Journal of Maritime Technology and Society. 2023 Feb 27:8-15. doi: https://doi.org/10.62012/mp.v2i1.25130

[9] A. alamsyah, A. Falevi, A. Wulandari, M. Pawara, W. Setiawan, and A. Arifuddin, "Investigating the Local Stress of Car Deck Ro-Ro 5000 GT", *EPI International Journal of Engineering*, vol. 4, no. 1, pp. 51-56, Feb. 2021. doi: https://doi.org/10.25042/epi-ije.022021.08

[10] Barsotti B, Battini C, Gaiotti M, Rizzo CM, Vergassola G. Experimental and numerical assessment of ultimate strength of a transversally loaded thin-walled deck structure. Marine Structures. 2025 Aug 15;103:103793. doi; https://doi.org/10.1016/j.marstruc.2025.103793

[11] K. Suzuki, "Safety margins and yielding criteria of service vessels based on classification rules," Journal of Marine Science and Engineering, vol. 9, no. 4, p. 412, 2021.

[12] A. M. N. Arifuddin, "Effect of Lifting Lug Hole Diameter Size on Strength Performance in Ship Block Lifting Process: English", *ISMATECH*, vol. 3, no. 1, Apr. 2025. doi: https://doi.org/10.35718/ismatech.v3i1.8481345

[13] A. I. Wulandari, R. J. Ikhwani, S. s. suardi, R. S. Yani, A. N. Himaya, and a. alamsyah, "Collision Analysis Of A Self Propelled Oil Barge (SPOB) Using Finite Element Method," *Kapal: Jurnal Ilmu*

Pengetahuan dan Teknologi Kelautan, vol. 19, no. 2, pp. 101-111, Jul. 2022. doi; https://doi.org/10.14710/kapal.v19i2.45417

[14] P. S. Lee and H. C. Noh, "A study on convergence criteria for four-node shell elements in ship midship modeling," International Journal for Numerical Methods in Engineering, vol. 102, no. 8, pp. 1420–1435, 2015.

[15] O. Hughes and J. K. Paik, Ship Structural Analysis and Design. Jersey City, NJ: SNAME, 2010.

[16] A. Alam, A. I. Wulandari, N. S. Oktavaro, M. U. Pawara, and M. Riyadi, "The Fatigue Life Assessment of Sideboard on Deck Barge Using Finite Element Methods", *Majalah Ilmiah Pengkajian Industri*, vol. 16, no. 1, pp. 1–10, Sep. 2023. doi: https://doi.org/10.29122/mipi.v16i1.5201

[17] Wang Y. Stochastic Dynamic Response and Stability of Ships and Offshore Platforms. Springer; 2024.

[18] M. U. Pawara, A. Pawara, M. Syarif, F. Mahmuddin, and Harifuddin, "Effect of Post Weld Heat Treatment on Tensile Strength of ASTM A36 Welded Joints: Application on Hull Vessel Material", *IJMEIR*, vol. 8, no. 1, pp. 56–65, Jul. 2025. doi: https://doi.org/10.12962/j25481479.v8i1

[19] Georgiadis DG, Samuelides ES, Straub D. A Bayesian analysis for the quantification of strength model uncertainty factor of ship structures in ultimate limit state. Marine Structures. 2023 Nov 1;92:103495. doi; https://doi.org/10.1016/j.marstruc.2023.103495

[20] Wulandari AI, Suardi A, Ciptiandi A. Strength analysis with variation of construction transverse watertight bulkhead on ship container 8842 dwt using finite element method. Int. J. Mar. Eng. Innov. Res. 2023 Jun 16;8. doi: https://doi.org/10.12962/j25481479.v8i2

[21] da Silveira T, Crestani EA, dos Santos ED, Isoldi LA. Numerical Analysis of Aspect Ratio Effects on the Mechanical Behavior of Perforated Steel Plates. Metals. 2025 Jul 11;15(7):786. doi; https://doi.org/10.3390/met15070786

[22] Han P, Pak C, Yun C, Ri K, Choe T. Empirical formulations for estimation of the ultimate strength of the perforated stiffened panels under the combined lateral pressure and in-plane compression. Ocean Engineering. 2022 Dec 15;266:112620. doi; 10.1016/j.oceaneng.2022.112620

[23] Y. N. Ivanov, "Load path redirection in structural optimization of ship hull modules," Marine Engineering Frontiers, vol. 8, no. 2, pp. 88–99, 2021.

[24] S. P. Timoshenko and S. Woinowsky-Krieger, Theory of Plates and Shells. New York, NY: McGraw-Hill, 1959.

[25] K. M. Rahman, "FEA simulation guidelines for structural behavior of tugboat hull panels," Ocean Systems Engineering, vol. 11, no. 3, pp. 245–259, 2021.

[26] M. S. Kim and J. M. Lee, "Weight optimization of small service vessels through framing arrangement modifications and finite element verification," Ocean Engineering, vol. 242, p. 110115, 2022.